Separation and Purification Technology 80 (2011) 643–651

Contents lists available at ScienceDirect

Separation and Purification Technology

journal homepage: www.elsevier.com/locate/seppur

Effects of alternating and direct current in electrocoagulation process on the removal of cadmium from water – A novel approach

Subramanyan Vasudevan *, Jothinathan Lakshmi

CSIR-Central Electrochemical Research Institute, Karaikudi 630 006, India

ARTICLE INFO

Article history:
Received 24 March 2011
Received in revised form 17 June 2011
Accepted 21 June 2011
Available online 26 June 2011

Keywords:
Electrocoagulation
Alternating/direct current
Cadmium removal
Adsorption kinetics
Isotherms

ABSTRACT

The main objective of this study is to investigate the effects of AC and DC on the removal of cadmium from water using zinc as anode and as cathode. Various operating parameters on the removal efficiency of cadmium were investigated, such as initial cadmium ion concentration, initial pH, current density and temperature. The results showed that the removal efficiency of 97.8% and 96.9% with the energy consumption of 0.665 and 1.236 kWh/m^3 was achieved at a current density of 0.2 A/dm^2 and pH of 7.0 using zinc as electrodes using AC and DC, respectively. For both AC and DC, the adsorption of cadmium was preferably fitting Langmuir adsorption isotherm, the adsorption process follows second order kinetics and the temperature studies showed that adsorption was exothermic and spontaneous in nature.

1. Introduction

It is well known that, heavy metals constitute a serious threat for the environment and human health, because they are not biodegradable and tend to accumulate in living organisms. Toxic heavy metals of particular concern in treatment of water include zinc, copper, nickel, mercury, cadmium, lead and chromium. These heavy metals, known as powerful toxic agents, are teratogenic and carcinogenic. Cadmium is one of the most toxic non-essential heavy metals present in the environment, even at low concentrations. Cadmium has been classified by US Environmental Protection Agency as a probable human carcinogen. Elevated level of cadmium ions arise from a variety of sources such as wastewater from metal plating industries, nickel–cadmium batteries, phosphate fertilizer, mining, pigments, stabilizers, alloys, petroleum refining, welding and pulp industries [1–3]. Cadmium poisoning includes kidney damage [4], lung insufficiency, cancer; it changes the constitution of bone, liver and blood [5]. Cadmium accumulated in the rice crops, it developed Itai–Itai disease and renal abnormalities including proteinuria and glucosuria. Cadmium containing compounds are known as carcinogens [6,7]. The drinking water guideline value is 0.005 mg/L [8].

Conventional methods for removing cadmium from water include ion exchange, reverse osmosis, co-precipitation, coagulation, complexation, solvent extraction, electrochemical treatment and adsorption [9–25]. Physical methods like ion exchange, reverse osmosis and electrodialysis have proven to be either too expensive or inefficient to remove cadmium from water. At present, chemical treatments are not used due to disadvantages like high costs of maintenance, problems of sludge handling and its disposal, and neutralization of the effluent [26]. The cadmium removal from water by adsorption using different materials has also been explored. The major disadvantages of this studied adsorbent are low efficiency and high cost. Recent research has demonstrated that electrocoagulation offers an attractive alternative to above-mentioned traditional methods for treating water [27]. In this process anodic dissolution of metal electrode takes place with the evolution of hydrogen gas at the cathode [28].

Electrochemically generated metallic ions from the anode can undergo hydrolysis to produce a series of activated intermediates that are able to destabilize the finely dispersed particles present in the water to be treated. The electrochemical reactions may be summarized as follows,

At anode,

$$Zn \rightarrow Zn^{2+} + 2e^- \quad (1a)$$

At cathode,

$$2H_2O_{(l)} + 2e^- \rightarrow H_{2(g)} + 2OH^- \quad (1b)$$

Overall,

$$Zn^{2+}(aq) + 2H_2O(l) \rightarrow Zn(OH)_2 \downarrow + 2H^+(aq) \quad (2)$$

The generated $Zn^{2+}_{(aq)}$ ions will immediately undergo further spontaneous reactions to produce corresponding hydroxides and/or polyhydroxides in a wide pH range. These hydroxides/

* Corresponding author. Tel.: +91 4565 227554; fax: +91 4565 227779.
E-mail address: svasudevan65@gmail.com (S. Vasudevan).

1383-5866/$ - see front matter © 2011 Elsevier B.V. All rights reserved.
doi:10.1016/j.seppur.2011.06.027

polyhydroxides/polyhydroxy metallic compounds have a strong affinity with dispersed/dissolved ions as well as the counter ions to cause coagulation/adsorption. The advantages of electrocoagulation include high particulate removal efficiency, a compact treatment facility, relatively low cost, and the possibility of complete automation. This method is characterized by reduced sludge production, a minimum requirement of chemicals and ease of operation [29–31].

In general, direct current (DC) is used in an electrocoagulation processes. In this case, an impermeable oxide layer may form on the cathode as well as corrosion formation on the anode due to oxidation. These prevent the effective current transport between the anode and cathode, so the efficiency of electrocoagulation processes declines. These disadvantages of DC have been overcome by adopting alternating current (AC) in electrocoagulation processes. The main objective of this study is to investigate the effect of AC on the removal efficiency of cadmium using zinc as anode and as cathode. The effect of the initial concentration of cadmium ion, pH, temperature, current density and coexisting ions were investigated. The adsorption kinetics of cadmium ions on zinc hydroxide is also studied. For this, equilibrium adsorption behavior is analyzed by fitting the Langmuir and Freundlich isotherm models. The adsorption kinetics of electrocoagulation was analyzed using first, second order kinetic models. Finally, the effects of temperature were studied to determine the nature of adsorption.

2. Materials and methods

2.1. Cell construction and electrolysis

The electrolytic cell consisting of a 1.0-L Plexiglas vessel (Fig. 1) that was fitted with a polycarbonate cell cover with slots to introduce the anode, cathode, pH sensor, a thermometer and electrolytes. Zinc (Commercial Grade, India) of surface area (0.02 m^2) acted as the anode and cathode and placed at an interelectrode distance of 0.005 m. The temperature of the electrolyte has been controlled to the desired value with a variation of ±2 K by adjusting the rate of flow of thermostatically controlled water through an external glass-cooling spiral. A regulated direct current (DC) was supplied from a rectifier (10 A, 0–25 V; Aplab model) and regulated alternating current (AC) was supplied from a source (0–5 A, 0–270 V, 50 Hz; AMETEK Model: EC1000S).

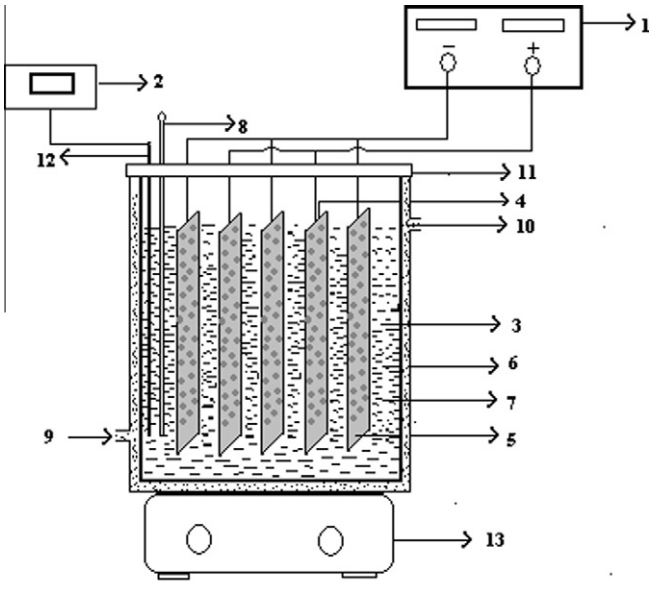

Fig. 1. Laboratory scale cell assembly. (1) DC power supply; (2) pH meter; (3) electrochemical cell; (4) cathodes; (5) anode; (6) electrolyte; (7) outer jacket; (8) thermostat; (9) inlet for thermostatic water; (10) outlet for thermostatic water; (11) PVC cover; (12) pH sensor and (13) magnetic stirrer.

Cadmium nitrate $Cd(NO_3)_2{\cdot}4H_2O$ (Analar Reagent, Merck, Germany) was dissolved in deionized water for the required concentration. In all the experiments 20 mg/L of cadmium was used. The pH of the electrolyte was adjusted, if required, with HCl or NaOH solutions before the electrolysis starts. To study the effect of co-existing ions, in the removal of cadmium, sodium salts (Analar Grade, Merck, Germany) of phosphate (0–50 mg/L), silicate (0–15 mg/L), carbonate (0–250 mg/L) and arsenate (0–5.0 mg/L) was added to the electrolyte. All the experiments were repeated three times for reproducibility and the accuracy of the results are ± 1%.

2.2. Analytical method

The concentration of cadmium was determined using UV–Visible Spectrophotometer with cadmium kits (MERCK, Pharo 300, Germany). The SEM and EDAX of cadmium adsorbed zinc hydroxide coagulant were analyzed with a Scanning Electron Microscope (SEM) made by Hitachi (model s-3000h). The Fourier transform infrared spectrum of zinc hydroxide was obtained using Nexus 670 FTIR spectrometer made by Thermo Electron Corporation, USA. The XRD for zinc hydroxide coagulant was analyzed by X-ray diffractometer made by JEOL X-ray diffractometer (Type – JEOL, Japan). The initial concentration of carbonate, phosphate, silicate and arsenate were determined using UV–Visible Spectrophotometer (MERCK, Pharo 300).

3. Results and discussion

3.1. Effect of current density

The current density is an important factor that strongly controls the reaction rate in most electrochemical processes, and it determines the coagulant dosage in the electrocoagulation process. The current density was determined by dividing each measured current by the corresponding electrode area. The amount of cadmium removal and removal rate has increased by increasing current density. Further, the amount of cadmium removal depends upon the quantity of adsorbent (zinc hydroxide) generated, which is related to the time and current density. To investigate the effect of current density on the cadmium removal, a series of experiments were carried out by solutions containing constant cadmium loading of 20 mg/L, at a pH 7.0, with current density being varied from 0.1 to 0.5 A dm^{-2} using both AC and DC current source. The results showed that the removal efficiency of 97.8% and 96.9% with the energy consumption of 0.665 and 1.236 kWh/m^3 was achieved at a current density of 0.2 A/dm^2 and pH of 7.0 using zinc as electrodes using AC and DC, respectively. The results are presented in Table 1. The results show that the removal efficiency of cadmium was higher and energy consumption was lower in the case of AC than DC. This may be due to the uniform dissolution of anode and cathode during electrocoagulation in the case of AC. The removal efficiency was shows that the amount of cadmium adsorption increases with the increase in adsorbent concentration, which indicates that the adsorption depends up on the availability of binding sites for cadmium.

3.2. Effect of pH

The pH is one of the important parameters affecting the performance of electrochemical process. In order to examine the effect of

Table 1
Effect of current density on the removal efficiency of cadmium using AC and DC with initial cadmium concentration 20 mg/L.

Current density (A/dm^2)	AC		DC	
	Removal efficiency (%)	Energy consumption (kWh/m^3)	Removal efficiency (%)	Energy consumption (kWh/m^3)
0.1	94.1	0.119	93.8	0.993
0.2	97.8	0.366	96.9	1.154
0.2	98.0	0.402	97.2	1.337
0.4	98.1	0.566	97.5	1.384
0.5	98.3	0.614	97.6	1.439

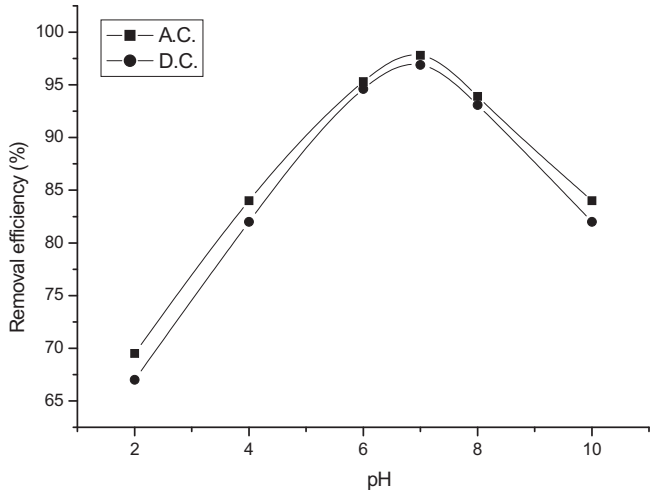

Fig. 2. Effect of pH of the electrolyte on the removal of cadmium. Conditions: electrolyte concentration of 20 mg/L; current density of 0.2 A/dm^2; temperature of 303 K.

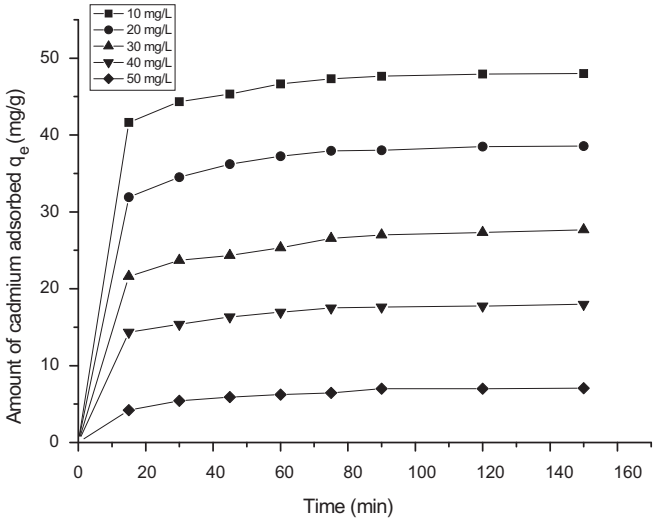

Fig. 3. Effect of electrolysis time and amount of cadmium adsorbed. Conditions: current density of 0.2 A/dm^2; pH of 7.0; temperature of 303 K.

the initial pH for AC and DC source, experiments were carried out in acidic (pH 2.0), slightly acidic (pH 5), neutral (pH 7.0), and alkaline (pH 10.0) media having 20 mg/L of cadmium containing solutions. The percentage of cadmium adsorption was maximum at pH 7, a decreasing trend in adsorption was observed when below and above pH 7 for both AC and DC source. At an initial concentration of 20 mg/L, maximum adsorption of 97.8% and 96.9% at pH 7 for AC and DC source, respectively was observed (Fig. 2). According to well known Zn–H_2O Pourbaix diagram [32] and in thermodynamic point of view, that the precipitation of $Zn(OH)_2$ would only be significant at pH $\geqslant$ 8.6, however, the interfacial pH-increase during the electrocoagulation process favored the zinc hydroxide formation and resulting higher removal efficiency at pH 7.0. At low pH, Cd^{2+} ions had to compete with H^+ ions for adsorption sites on the adsorbent surface. As the pH increased, this competition weakens and more Cd^+ ions were able to replace H^+ ions bound to the adsorbent surface.

3.3. Effect of initial cadmium concentration

To study the effect of initial concentration, experiments were conducted at varying initial concentrations from 10–50 mg/L using AC and DC. The removal of Cd increased with time to obtain equilibrium at about 30 min (Fig. 3). The amount of cadmium adsorbed (q_e) increased from 6.37 to 48.21 mg/g as the concentration was increased from 10 to 50 mg/L for the AC source. The figure also shows that the adsorption is the rapid in the initial stages and gradually decreases with progress of adsorption this is because of the great number of sites available for the sorption operation and adsorption equilibrium were then gradually achieved. The plots are single, smooth and continuous curves leading to saturation, suggesting the possible monolayer coverage to cadmium on the surface of the adsorbent [33]. In the case of DC the equilibrium time was found to be 50 min for all concentration studied (figure not shown).

3.4. Effect of coexisting ions

To study the effect of co-existing ions, in the removal of cadmium, sodium salts of carbonate (0–250 mg/L), phosphate (0–50 mg/L), silicate (0–15 mg/L), and arsenate (0 5.0 mg/L) was added to the electrolyte and electrolysis was carried out using AC with an initial pH of 7.

3.4.1. Carbonate

Effect of carbonate on cadmium removal was evaluated by increasing the carbonate concentration from 2 to 250 mg/L in the electrolyte. The removal efficiencies are 97.8%, 97.7%, 80%, 69.1%, 30.2%, and 16% for the carbonate ion concentration of 0, 2, 5, 65, 150 and 250 mg/L, respectively. From the results it is found that the removal efficiency of the cadmium is not affected by the presence of carbonate below 5 mg/L. Significant reduction in removal efficiency was observed above 5 mg/L of carbonate concentration is due to the passivation of anode resulting, the hindering of the dissolution process of anode. It is also observed that, at higher concentrations of carbonate the energy consumption was higher due to anode passivation (Table 2).

3.4.2. Phosphate

The concentration of phosphate ion was increased from 2 to 50 mg/L, the contaminant range of phosphate in the ground water. The removal efficiency for cadmium was 97.8%, 97.8%, 71.3%, 52.6% and 43% for 0, 2, 5, 25 and 50 mg/L of phosphate ion, respectively.

Table 2
Effects of co-existing ions on the removal of cadmium from water with AC source with initial cadmium concentration 20 mg/L.

Concentration (mg/L)	Voltage (V)	Removal efficiency (%)	Energy consumption (kWh/m^3)
Carbonate			
Nil	1.5	97.8	1.154
2.0	1.7	97.08	1.158
5.0	2.2	80.0	1.496
65.0	3.4	69.1	2.380
150.0	4.0	30.2	2.721
250.0	5.7	16.0	3.876
Phosphate			
Nil	1.5	97.8	1.154
2.0	1.6	97.8	1.155
5.0	1.8	71.3	1.224
25.0	2.0	52.60	1.360
50.0	2.6	43.0	1.768
Silicate			
Nil	1.5	97.8	1.154
2.0	1.7	97.0	1.158
5.0	1.8	65.0	1.224
10.0	2.3	46.0	1.564
15.0	2.6	19.0	1.768
Arsenate			
Nil	1.5	97.8	1.154
0.5	1.5	81.2	1.154
1.0	1.5	70.2	1.154
3.0	1.9	64.0	1.292
5.0	2.0	31.0	1.360

The results are presented in Table 2. There is no change in removal efficiency of cadmium below 5 mg/L of phosphate in the water. At higher concentrations (at and above 5 mg/L) of phosphate, the removal efficiency decreases to 43%. This is due to the preferential adsorption of phosphate over cadmium as the concentration of phosphate increase.

3.4.3. Silicate

Effect of different concentrations of silicate on the removal efficiency of cadmium was investigated. The respective efficiencies for 0, 2, 5, 10 and 15 mg/L of silicate are 97.8%, 97%, 65%, 46% and 19%. The removal of cadmium decreased with increasing silicate concentration from 0 to 15 mg/L (Table 2). In addition to preferential adsorption, silicate can interact with zinc hydroxide to form soluble and highly dispersed colloids that are not removed by normal filtration.

3.4.4. Arsenate

Effect of arsenate on cadmium removal was evaluated by increasing the arsenate concentration from 0 to 5 mg/L in the electrolyte. From the results (Table 2) it is found that the efficiency decreased from 97.8%, 81.2%, 70.2%, 64–31% by increasing the concentration of arsenate from 0, 0.5,1,3 and 5 mg/L. Like phosphate ion, this is due to the preferential adsorption of arsenic over cadmium as the concentration of arsenate increases. So, when arsenic ions present in the water are to be treated which compete greatly with cadmium ions for the binding sites.

3.5. Adsorption kinetics

In the present investigation, two kinetic models, namely, first order and second order models were tested to obtain rate constants, equilibrium adsorption capacity, and adsorption mechanism at different concentrations. The adsorption of cadmium is analyzed using first order Lagergren model [34,35].

$$dq/dt = k_1(q_e - q_t) \quad (3)$$

where, q_t is the amount of cadmium adsorbed on the adsorbent at time t (min) and k_1 (1/min) is the rate constant of first order adsorption. The integrated form of the above equation with the boundary conditions $t = 0$ to $t > 0$ ($q = 0$ to $q > 0$) and then rearranged to obtain the following time dependence function,

$$\log(q_e - q_t) = \log(q_e) - k_1 t/2.303 \quad (4)$$

where q_e is the amount of cadmium adsorbed at equilibrium. The q_e and rate constant (k_1) were calculated from the slope of the plots of log ($q_e - q_t$) versus time (t) (figure not shown). It is found that, the shape of the lines obtained from the plot of log ($q_e - q_t$) versus t at different concentrations indicated that the first-order Lagergren equation did not fit well to the experimental data at all concentrations. It is also found that the calculated q_e value do not agrees with the experimental q_e values. It is thus inappropriate to use the Lagergren kinetic model to predict the sorption kinetics of cadmium on zinc hydroxide.

Further, the kinetic data was fitted to the second-order equation as [36].

$$dq/dt = k_2(q_e - q_t)^2 \quad (5)$$

where k_2 is the rate constant of second order adsorption. The integrated form of Eq. (5) with the boundary condition $t = 0$ to $t > 0$ ($q = 0$ to $q > 0$) is

$$1/(q_e - q_t) = 1/q_e + k_2 t \quad (6)$$

Eq. (7) can be rearranged and linearized as,

$$t/q_t = 1/k_2 q_e^2 + t/q_e \quad (7)$$

The linear plots of t/q_t versus time (t) at different concentrations are shown in Fig. 4. The second order kinetic values of q_e and k_2 were calculated from the slope and intercept of the plots t/q_t versus t. Table 3 depict the computed results obtained from first and second order kinetic model for AC and DC source. An analysis of the data in Table 3 suggests that the kinetics of adsorption of cadmium on zinc hydroxide can be explained accurately by the second-order kinetic model. The calculated q_e values were found to be quite close to the experimental q_e values at all the concentrations studied (10–50 mg/L) for AC and DC source. So, it is inferred that the adsorption of cadmium on zinc hydroxide followed second-order kinetics.

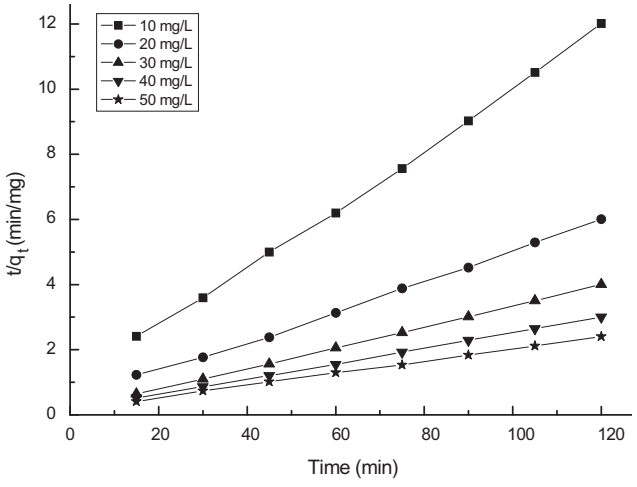

Fig. 4. Second order kinetic model plot of different concentrations of cadmium. Conditions: current density of 0.2 A/dm^2; temperature of 303 K; pH of 7.0.

Table 3
Comparison between the experimental and calculated q_e values for different initial cadmium concentrations in first and second order adsorption kinetics at temperature 305 K and pH 7.

Current source	Concentration (mg/L)	q_e (exp)	First order adsorption			Second order adsorption		
			q_e (Cal)	$k_1 \times 10^3$ (min/mg)	R^2	q_e (Cal)	$k_2 \times 10^3$ (min/mg)	R^2
AC	10	6.37	36.24	−0.0038	0.7966	6.33	2.021	0.9999
	20	15.22	40.22	−0.0041	0.7941	15.12	4.566	0.9986
	30	24.01	49.36	−0.0056	0.8066	23.82	6.574	0.9994
	40	34.69	59.44	−0.0078	0.7843	34.19	6.816	0.9990
	50	48.21	61.73	−0.0133	0.8124	47.86	6.994	0.9988
DC	10	6.29	30.55	−0.0031	0.7615	6.26	2.115	0.9996
	20	15.13	47.55	−0.0037	0.7934	15.01	4.021	0.9952
	30	23.96	54.32	−0.0041	0.7861	23.88	5.231	0.9994
	40	34.54	56.61	−0.0045	0.7998	34.36	5.662	0.9986
	50	47.93	57.34	−0.0054	0.8013	47.82	5.836	0.9993

3.6. Adsorption isotherm

An adsorption isotherm represents the equilibrium relationship between the adsorbate concentration in the liquid phase and that on the adsorbent's surface at a given condition. A number of isotherms have been developed to describe equilibrium relationships. In the present study, the Freundlich, Langmuir and Dubinin–Radushkevich (D–R) models were used to describe the equilibrium data. To determine the isotherms, the initial pH was kept at 7 and the concentration of cadmium used was in the range of 10–50 mg/L.

3.6.1. Freundlich isotherm

The mathematical expression of the Freundlich model can be written as [37].

$$q_e = K_c^n \tag{8}$$

Eq. (8) can be linearized in logarithmic form and the Freundlich constants can be determined as follows [38]

$$\log q_e = \log k_f + n \log C_e \tag{9}$$

where k_f is the Freundlich constant related to adsorption capacity, 'n' is the energy or intensity of adsorption, C_e is the equilibrium concentration of cadmium. To determine the isotherms, the cadmium concentration used was 10–50 mg/L and at an initial pH 7. The Freundlich constants 'k_f' and 'n' values for AC and DC source were shown in Table 4. It has been reported that values of 'n' lying between 0 and 1 indicate favorable adsorption. From the analysis of the results it is found that the Freundlich plots fit satisfactorily with the experimental data obtained in the present study.

3.6.2. Langmuir isotherm

The linearized form of Langmuir adsorption isotherm model is [39].

$$C_e/q_e = 1/q_o b + C_e/q_o \tag{10}$$

where C_e is the concentration of the cadmium solution (mg/L) at equilibrium, q_o is the adsorption capacity (Langmuir constant) and b is the energy of adsorption. Fig. 5 shows the Langmuir plot with experimental data. Langmuir plot is a better fit with the experimental data compare to Freundlich plots. The value of the adsorption capacity q_m as found to be 501.31 mg/g and 490.22 mg/g for AC and DC source. The essential characteristics of the Langmuir isotherm can be expressed as the dimensionless constant R_L [40]

$$R_L = 1/(1 + bc_o) \tag{11}$$

where R_L is the equilibrium constant it indicates the type of adsorption, b, C_o is the Langmuir constant. The R_L values between 0 and 1 indicate the favorable adsorption (Table 4).

3.6.3. Dubinin–Radushkevich (D–R) isotherm

The D–R model, which does not assume a homogeneous surface or a constant adsorption potential as the Langmuir model, is used to test the equilibrium data and to estimate the mean free energy of adsorption (E). This model is given by,

$$q_e = q_s \exp(-B\varepsilon^2) \tag{12}$$

where ε is Polanyi potential, equal to RT ln (1 + 1/C_e), B is related to the free energy of sorption and q_s is the Dubinin–Radushkevich (D–R) isotherm constant [41]. The linearized form is,

$$\ln q_e = \ln q_s - 2BRT \ln [1 + 1/C_e] \tag{13}$$

The isotherm constants of q_s and B are obtained from the intercept and slope of the plot of ln q_e versus ε^2 [42]. The constant 'B' gives the mean free energy of adsorption per molecule of the adsorbate when it is transferred from the solid from infinity in the solution and the relation is given as

$$E = [1/\sqrt{2B}] \tag{14}$$

Table 4
Constant parameters and correlation co-efficient calculated for different adsorption isotherm models for cadmium adsorption at 20 mg/L at room temperature.

Isotherm	Constants				
Langmuir		q_m (mg/g)	b (L/mg)	R_L	R^2
	AC	501.31	0.0027	0.8455	0.9998
	DC	490.22	0.0019	0.8625	0.9989
Freundlich		K_f (mg/g)	n (L/mg)		R^2
	AC	1.441	1.112		0.9847
	DC	1.236	1.039		0.9864
D–R		Q_s ($\times 10^3$ mol/g)	B ($\times 10^3$ mol^2/kJ^2)	E (kJ/mol)	R^2
	AC	0.477	0.2663	6.99	0.8421
	DC	0.489	0.2745	6.21	0.8346

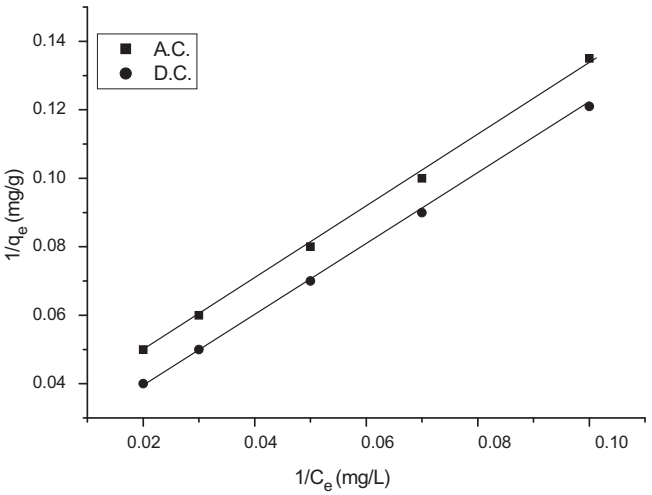

Fig. 5. Langmuir plot ($1/C_e$ Vs $1/q_e$). Conditions: pH of 7.0; current density: 0.2 A/dm^2; temperature of 303 K; concentration of 10–50 mg/L.

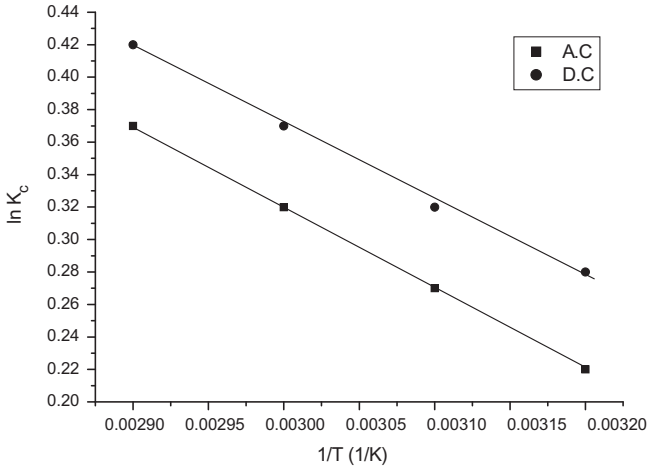

Fig. 6. Plot of ln K_c and $1/T$. Conditions: pH of 7.0; current density of 0.2 A/dm^2; temperature of 303 K; concentration of 10–50 mg/L.

Table 5
Pore diffusion coefficients for the adsorption of cadmium at various concentrations and temperature.

	Pore diffusion constant $D \times 10^{-9}$ (cm^2/s)
Concentration (mg/L)	
10	1.2211
20	0.9736
30	0.9561
40	0.9366
50	0.9178
Temperature (K)	
313	0.9744
323	1.0215
333	1.4067
343	1.9825

The magnitude of E is useful for estimating the type of adsorption process. It was found to be 6.99 and 6.21 kJ/mol for AC and DC, which is smaller than the energy range of adsorption reaction, 8–16 kJ/mol [43]. So the type of adsorption of cadmium on zinc hydroxide was defined as chemical adsorption.

The correlation co-efficient values of different isotherm models are listed in Table 4. The Langmuir isotherm model has higher regression co-efficient (R^2 = 0.999) when compared to the other models. The adsorption data show good fit to the Langmuir then Freundlich and D–R adsorption isotherm as depicted by the regression coefficient for these systems for both AC and DC. R_L values between 0 and 1 further indicate a favorable adsorption of cadmium.

3.7. Effect of temperature

The effect of temperature for adsorption of cadmium on zinc hydroxide was investigated at four different temperatures (313–343 K). The amount of cadmium adsorbed on the adsorbent increases by increasing the temperature indicating the process to be endothermic. The diffusion co-efficient (D) for intraparticle transport of cadmium species into the adsorbent particles has been calculated at different temperature by

$$t_{1/2} = 0.03 \times r_o^2/D \quad (15)$$

where $t_{1/2}$ is the time of half adsorption (s), 'r_o' is the radius of the adsorbent particle (cm), D is the diffusion co-efficient in cm^2/s. For all chemisorption system the diffusivity co-efficient should be 10^{-5}–10^{-13} cm^2/s [44]. In the present work, D is found to be in the range of 10^{-9}cm^2 /s. The pore diffusion coefficient (D) values for various temperatures and different initial concentrations of cadmium are presented in Table 5.

To find out the energy of activation for adsorption of cadmium, the second order rate constant is expressed in Arrhenius form [45].

$$\ln k_2 = \ln k_o - E/RT \quad (16)$$

where k_o is the constant of the equation (g/mg/min), E is the energy of activation (J/mol), R is the gas constant (8.314 J/mol K) and T is the temperature in K. The activation energy (7.335 kJ/mol for AC and 5.62 kJ/mol for DC source) is calculated from slope of the fitted equation. The free energy change is obtained using the following relationship:

$$\Delta G = -RT\ln K_c \quad (17)$$

where ΔG is the free energy (kJ/mol), K_c is the equilibrium constant, R is the gas constant and T is the temperature in K. The K_c and ΔG values are presented in Table 6. From the table it is found that the negative value of ΔG indicates the spontaneous nature of adsorption. Other thermodynamic parameters such as entropy change (ΔS) and enthalpy change (ΔH) were determined using van't Hoff equation,

Table 6
Thermodynamic parameters for the adsorption of cadmium.

Temperature (K)	AC				DC			
	K_c	ΔG^o (J/mol)	ΔH^o (kJ/mol)	ΔS^o (J/mol K)	K_c	ΔG^o (J/mol)	ΔH^o (kJ/mol)	ΔS^o (J/mol K)
313	1.0068	−0.1122			0.9989	−0.0662		
323	1.146	−0.1279			1.0661	−0.0864		
333	1.1635	−0.1946	8.445	10.338	1.1151	−0.1764	8.669	9.836
343	1.1742	−0.2678			1.1364	−0.1982		

Table 7
Comparison between the experimental and calculated q_e values for different initial cadmium concentrations of 20 mg/L in first and second order adsorption kinetics at various temperatures and pH 7.

Temperature (K)	q_e (exp)	First order adsorption			Second order adsorption		
		q_e (Cal)	K_1(min/mg)	R^2	q_e (Cal)	K_2 (min/mg)	R^2
313	15.22	26.34	−0.0016	0.7866	15.14	0.1126	0.9999
323	15.36	32.15	−0.0029	0.7946	15.28	0.1637	0.9986
333	15.49	38.61	−0.0036	0.8103	15.36	0.2865	0.9975
343	15.62	40.36	−0.0042	0.7632	15.55	0.3346	0.9964

$$\ln K_c = \frac{\Delta S}{R} - \frac{\Delta H}{RT} \quad (18)$$

The enthalpy change and entropy change were obtained from the slope and intercept of the van't Hoff linear plots of ln K_c versus $1/T$ (Fig. 6). A positive value of enthalpy change (ΔH) indicates that the adsorption process is endothermic in nature, and the negative value of change in internal energy (ΔG) show the spontaneous adsorption of cadmium on the adsorbent. Positive values of entropy change show the increased randomness of the solution interface during the adsorption of cadmium on the adsorbent. Enhancement of adsorption capacity of electro coagulant (zinc hydroxide) at higher temperatures may be attributed to the enlargement of pore size and or activation of the adsorbent surface. Using Lagergran rate equation, first order rate constants and correlation co-efficient were calculated for different temperatures (313–343 K). The calculated 'q_e' values obtained from the first order kinetics agrees with the experimental 'q_e' values better than the second order kinetics model. Table 7 depicts the computed results obtained from first and second order kinetic models. These results indicate that the adsorption follows first order kinetic model at different temperatures used in this study. From the table, it is found that the rate constant 'k_2' increased with increasing the temperature from 305 to 343 K. The increase in adsorption may be due to change in pore size on increase in kinetic energy of the zinc species and the enhanced rate of intraparticle diffusion of adsorbate.

3.8. A pilot plant study

A pilot plant capacity cell (Fig. 7) was designed, fabricated and operated for the removal of cadmium from water. The system consists of AC/DC power supply, an electrochemical reactor, a water tank, a feed pump, a flow control valve, a flow measuring unit, a circulation pump, settling tank, filtration unit provisions for gas outlet and treated water outlet. The reactor is made of PVC with an active volume of 3000 L. The zinc electrodes (anode and cathode) each consist of five pieces situated approximately 5 mm apart from each other and submerged in the solution. The total electrode surface area is 1500 cm^2 for both cathodes and anodes. The cell was operated at a current density of 0.2 A/dm^2 and the electrolyte pH of 7.0. The results showed that the removal efficiency of 97.8% and 96.9% with the energy consumption of 0.665 and 1.236 kWh/m^3 was achieved at a current density of 0.2 A dm^{-2} and pH of 7.0 using zinc as electrodes using AC and DC, respectively. The results were consistent with the results obtained from the laboratory scale, showing that the process was technologically feasible.

From the above results it is found that the energy consumption is higher in the case of alternating current than direct current for the removal of cadmium from water. This is because, alternating current is helpful to prevent the passivation of Zn anode during the electrolysis and avoid the extra energy consumption for resistance of zinc oxide film formed on the anode surface. The SEM images of Zn electrodes after electrolysis in cadmium

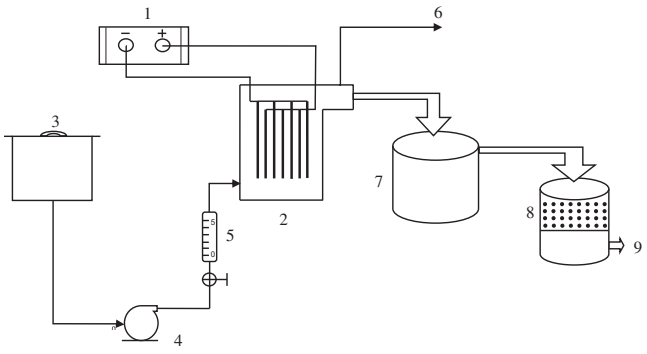

Fig. 7. Flow diagram of the pilot plant electrocoagulation system. (1) DC power supply, (2) electro coagulation cell, (3) water tank, (4) inlet pump, (5) flow meter, (6) gas outlet, (7) setting tank, (8) filter and (9) treated water.

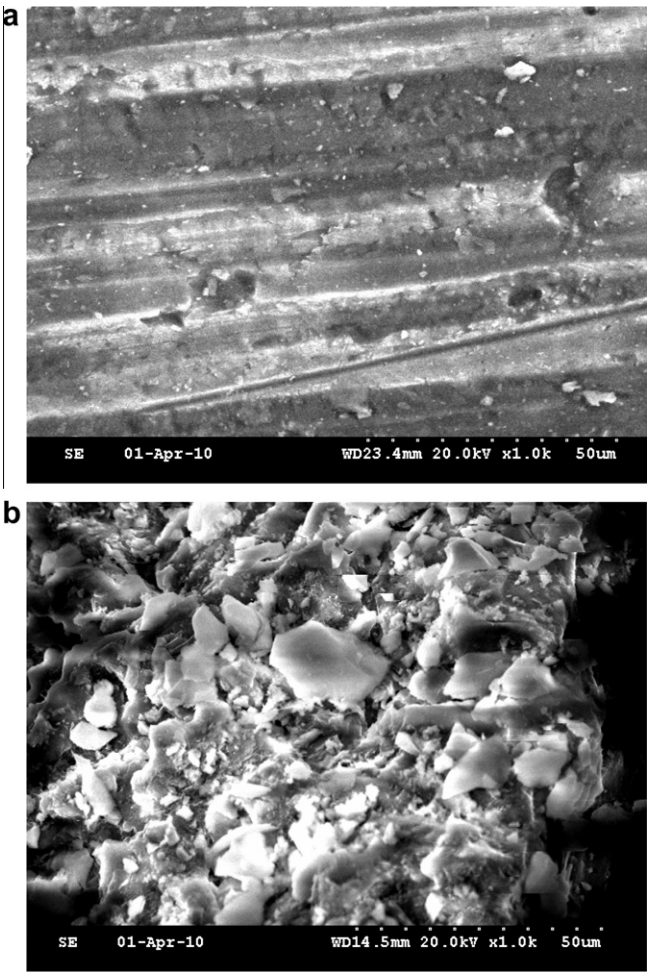

Fig. 8. SEM images of the anode after electrocoagulation by (a) AC and (b) DC.

contaminated water showed that Zn was dissolved uniformly during alternating current electrocoagulation and less oxide formed on the surface during the electrolysis.

3.9. Surface characterization

3.9.1. SEM and EDAX characterization

In order to gain more insight into the effect of alternating current, the morphology of the electrode surface after two kinds of electrolysis (AC and DC) was characterized by SEM as shown in Fig. 8(a) and (b). It can be observed that when the AC was fed, less disordered pores formed and a smooth microstructure of zinc suggesting the zinc electrodes were dissolved uniformly during the electrolysis. While for the electrodes fed with DC, the electrode surface is found to be rough, with a number of dents. These dents are formed around the nucleus of the active sites where the electrode dissolution results in the production of zinc hydroxides. The formation of a large number of dents may be attributed to the anode material consumption at active sites due to the generation of oxygen at its surface.

Energy-dispersive analysis of X-rays was used to analyze the elemental constituents of cadmium-adsorbed zinc hydroxide (Fig. 9). It shows that the presence of cadmium, Zn and O appears in the spectrum. EDAX analysis provides direct evidence that cadmium is adsorbed on zinc hydroxide.

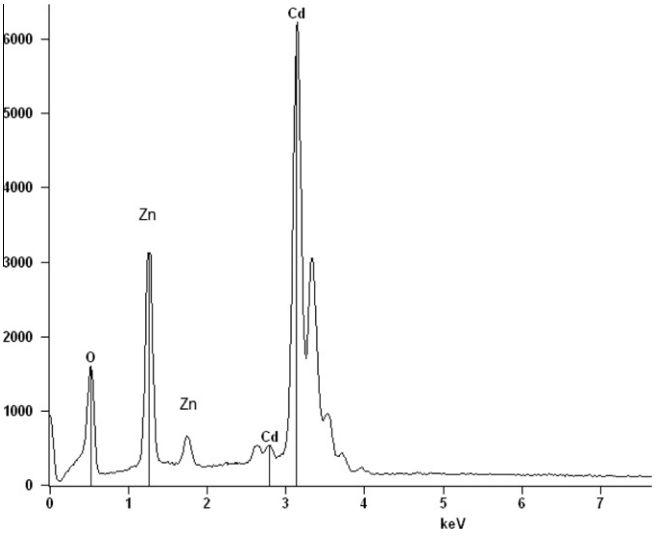

Fig. 9. EDAX spectrum of cadmium-adsorbed zinc hydroxide.

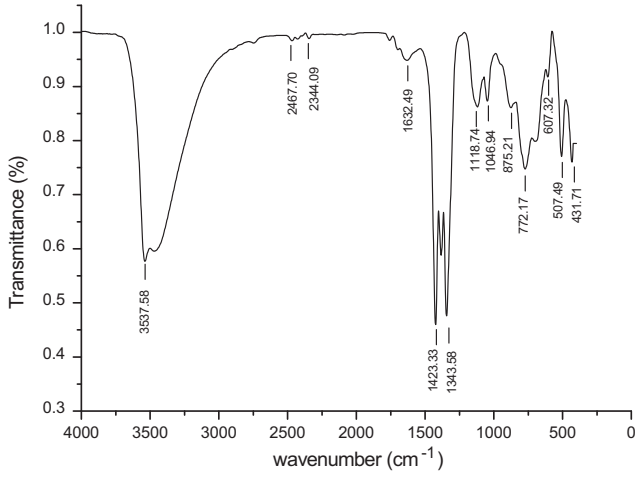

Fig. 10. FTIR spectrum of cadmium adsorbed zinc hydroxide.

3.9.2. FTIR and XRD studies

Fig. 10 presents the FT–IR spectrum of cadmium–zinc hydroxide. The sharp and strong peak at 3537.58 cm^{-1} is due to the O–H stretching vibration in the $Zn(OH)_2$ structures. The 1632.49 cm^{-1} peak indicates the bent vibration of H–O–H. The strong peak at 1046.94 cm^{-1} is assigned to the Zn–O–H bending. Cd–O vibration at 875.21 cm^{-1} also observed. The XRD spectrum of electrocoagulant (figure not shown), from the figure it is found that the electrocoagulation-by product showed the well crystalline phase of zinc hydroxide.

4. Conclusion

The results showed that the optimum removal efficiency of cadmium is 97.8% and 96.9% with the energy consumption of 0.665 and 1.236 kWh/m^3 was achieved for AC and DC source at a current density of 0.2 A/dm^2 and pH of 7.0 using zinc as anode and cathode. The results of the pilot scale study indicate that the process can be scaled up to higher capacity. For both AC and DC electrolysis the adsorption of cadmium preferably fitting Langmuir adsorption isotherm. The adsorption process follows second order kinetics. Temperature studies showed that adsorption was endothermic and spontaneous in nature. From the surface characterization studies, it is confirmed that the zinc hydroxide generated in the cell adsorbed cadmium present in the water.

Acknowledgment

The authors wish to express their gratitude to the Director, Central Electrochemical Research Institute, Karaikudi to publish this paper.

References

[1] O.J. Nrlagu, M.J. Pacyna, Quantitative assessment of worldwide contamination of air water and soils by trace metals, Nature 333 (1988) 134–139.
[2] M. Tsezos, Biosorption of metals. The experience accumulated the outlook for technology development, Hydrometallurgy 59 (2001) 241–243.
[3] K. Bedow, I. Bekri-Abbes, E. Srasra, Removal of cadmium (II) from aqueous solution using pure Smectite and Lewatite S 100: the effect of time and metal concentration, Desalination 223 (2008) 269–273.
[4] K. Nogawa, E. Kobayashi, Y. Okubo, Y. Suwazono, Environmental cadmium exposure adverse effects and preventive measures in Japan, Biometals 17 (2008) 581–587.
[5] H.A. Schroede, Cadmium as a factor in hypertension, J. Chronic Dis. 18 (1965) 647–656.
[6] T.H. Bui, J. Lindsten, G.F. Nordberg, Chromosome analysis of lymphocytes from cadmium workers and Itai–Itai patients, Environ. Res. 9 (1975) 187–195.
[7] IARC, beryllium, cadmium, mercury and exposures in the glass manufacturing industry monographs on the evaluation of carcinogenic. Risks to Humans 58 (1994) 444–447.
[8] Central Pollution Control Board, Ministry of Environment and Forests, Govt. of India, Delhi, Available from: <http://www.cpcb.nic.in>.
[9] D.G. Kinniburgh, M.L. Jackson, in: M.A. Anderson, A.J. Rubin (Eds.), Adsorption of Organics at Solid–Liquid Interfaces, Ann Arbor Science Publishers, Ann Arbor, MI, 1981, p. 91.
[10] M.S. Rahman, M.R. Islam, Adsorption of Cd(II) ions from synthetic waste water using maple sawdust, Energy Sources Part A 32 (2010) 222–231.
[11] S.C. Ibrahim, M.A.K. Hanafiah, M.Z.A. Yahya, Removal of cadmium from aqueous solutions by adsorption onto sugarcane, Am. Eur. J. Agri. Environ. Sci. 3 (2006) 179–187.
[12] M.A.K. Megat Hanafiah, M.Z.A. Yahya, H. Zakaria, S.C. Ibrahim, Adsorption of Cd(II) ions from aqueous solutions by Lalang (*Imperata cylindrica*) leaf powder: effect of physiochemical environment, J. Appl. Sci. 7 (2007).
[13] A. Archana, K.K. Sahu, Kinetic and isotherm studies of cadmium adsorption on manganese nodule residue, J. Hazard. Mater. 137 (2007) 915–922.
[14] E.J. Chou, Y. Okamoto, Removal of cadmium ion from aqueous solutions, J. Water. Poll. Control. Fed. 48 (1976) 2747–2753.
[15] J.K. Salpathy, M. Chaudhuri, Treatment of cadmium-plating and chromium-plating wastes by iron-coated sand, Water Environ. Res. 67 (1995) 788–790.

[16] C.A. Cristophi, L. Axe, Competition of Cd, Cu and Pb adsorption on goethite, J. Environ. Eng 126 (2000) 67–73.
[17] J.L. Gardea-Torresdey, G. de la Rosa, J.R. Peralta-Videa, Use of phytofiltration technologies in the removal of heavy metals: a review, Pure Appl. Chem. 76 (2004) 801–813.
[18] M. Ajmal, R.A. Rao, S. Anwar, J. Ahmad, R. Ahmad, Adsorption studies on rice husk: removal and recovery of Cd (II) from wastewater, Biosource. Tech. 86 (2003) 147–149.
[19] W.S. Peternele, A.A. Winkler-Hechenleitner, E.A. GomezPineda, Adsorption of Cd (II) and Pb (II) on to functionalized formic lignin from sugar cane bagasse, Bioresource Tech. 68 (1999) 95–100.
[20] A. Saeed, M. 1qbal, Bioremoval of cadmium from aqueous solution by gram husk, Water Res. 37 (2003) 3472–3482.
[21] D.P. Tiwari, D.K. Singh, D.N. Saksena, Removal of cadmium from wastewater, J. Environ. Eng. 121 (1995) 479–484.
[22] W.E. Marshall, M. Johns, Agricultural by-products as metal adsorbents: sorption properties and resistance to mechanical abrasion, J. Chem. Tech. Biotech. 66 (1996) 192–198.
[23] I.B. Abbes, S. Bayoudh, M. Baklouti, Converting waste polystyrene into adsorbent: Potential use in the removal of lead and cadmium ions from aqueous solution, J. Polym. Environ. 14 (2006) 249–256.
[24] S.I. Haider Taqvi, S.M. Hasany, M. Iqbal Bhanger, Sorption profile of Cd(II) ions onto beach sand from aqueous solutions, J. Hazard. Mater. 141 (2007) 37–44.
[25] S. Kocaoba, G. Akcin, Removal of chromium (III) and cadmium (II) from aqueous solutions, Desalination 180 (2005) 151–156.
[26] S. Vasudevan, J. Lakshmi, J. Jayaraj, G. Sozhan, Remediation of phosphate – contaminated water by electrocoagulation with aluminium, aluminium alloy and mild steel anodes, J. Hazard. Mater. 164 (2009) 1480–1486.
[27] X. Chen, G. Chen, P.L. Yue, Investigation on the electrolysis voltage of electrocoagulation, Chem. Eng. Sci. 57 (2002) 2449–2455.
[28] J.Q. Jiang, N. Graham, C. André, G.H. Kelsall, N. Brandon, Laboratory study of electro-coagulation-flotation for water treatment, Water Res. 36 (2002) 4064–4078.
[29] S. Vasudevan, S. Margrat Sheela, J. Lakshmi, G. Sozhan, Optimization of the process parameters for the removal of boron from drinking water by electrocoagulation – a clean technology, J. Chem. Technol. Biotech. 85 (2010) 926–933.
[30] S. Vasudevan, G. Sozhan, S. Ravichandran, J. Jayaraj, J. Lakshmi, S. Margrat Sheela, Studies on the removal of phosphate from drinking water by electrocoagulation process, Ind. Eng. Chem. Res. 47 (2008) 2018–2023.
[31] G. Chen, Electrochemical technologies in wastewater treatment, Sep. Purif. Technol. 38 (2004) 11–41.
[32] J. Vanmuylder, M. Pourbaix, In atlas of electrochemical equilibria in: J. Vanmuylder, M. Pourbaix (Eds.), Aquous Solutions: Zinc, Pergamon, New York, 409, 1966pp.
[33] K. Nadhem Hamadi, Xiao Dong Chen, M. Mohammed Farid, G.Q. Max Lu, Adsorption kinetics for the removal of chromium(VI) from aqueous solution by adsorbents derived from used tyres and sawdust, Chem. Eng. J. 84 (2001) 95–105.
[34] M.S. Gasser, G.H.A. Morad, H.F. Aly, Batch kinetics and thermodynamics of chromium ions removal from waste solutions using synthetic adsorbents, J. Hazard. Mater. 142 (2007) 118–129.
[35] F.H. Uber, Die adsorption in Losungen, Z. Phy. Chem 57 (1985) 387–389.
[36] C. Namasivayam, K. Prathap, Recycling Fe(III)/Cr(III) hydroxide, an industrial solid waste for the removal of phosphate from water, J. Hazard. Mater. 123B (2005) 127–135.
[37] I. Langmuir, The adsorption of gases on plane surfaces of glass, mica and platinum, Am. Chem. Soc. 40 (1918) 1361–1403.
[38] L. Michelson, P.G. Gideon, E.G. Pace, L.H. Kutal, Office of Water Research and Technology Bulletin 265 (1965).
[39] H. Demiral, I. Demiral, F. Tumsek, B. Karacbacakoglu, Adsorption of chromium(Vl) from aqueous solution by activated carbon derived from olive bagasse and applicability of different adsorption models, Chem. Eng. J. 144 (2008) 184–188.
[40] E. Oguz, Adsorption characteristics the kinetics of the Cr(VI) on the *Thuja oriantalis*, Colloid. Surf. 252 (2005) 121–128.
[41] I.A.W. Tan, B.H. Hameed, A.L. Ahmed, Equilibrium and kinetic studies on basic dye adsorption by oil palm fibre activated carbon, Chem. Eng. J. 127 (2007) 11–119.
[42] X.Y. Yang, B. Al-Duri, Application of branched pore diffusion model in the adsorption of reactive dyes on activated carbon, Chem. Eng. J. 83 (2001) 15–23.
[43] A.K. Golder, A.N. Samantha, S. Ray, Removal of phosphate from aqueous solution using calcined metal hydroxides sludge waste generated from electrocoagulation, Sep. Purif. Technol. 52 (2006) 102–108.
[44] M. Yurdakoc, Y. Seki, S. Karahan, K. Yurdakoc, Kinetic and thermodynamic studies of boron removal by Siral 5, Siral 40, and Siral 80, J. Colloid Interface Sci. 286 (2005) 440–446.
[45] S. Vasudevan, J. Lakshmi, G. Sozhan, Studies on the removal of iron from drinking water by electrocoagulation – a clean process, Clean 37 (2009) 45–51.